Published for SISSA by Springer

Two-loop integral reduction from elliptic and hyperelliptic curves

Alessandro Georgoudis and Yang Zhang

ETH Zürich, Institute for Theoretical Physics,
Wolfgang-Pauli-Str. 27, 8093 Zürich, Switzerland

E-mail: georgoua@student.ethz.ch, yang.zhang@phys.ethz.ch

ABSTRACT: We show that for a class of two-loop diagrams, the on-shell part of the integration-by-parts (IBP) relations correspond to exact meromorphic one-forms on algebraic curves. Since it is easy to find such exact meromorphic one-forms from algebraic geometry, this idea provides a new highly efficient algorithm for integral reduction. We demonstrate the power of this method via several complicated two-loop diagrams with internal massive legs. No explicit elliptic or hyperelliptic integral computation is needed for our method.

Contents

1 Introduction

With the beginning of Run II of the Large Hadron Collider (LHC), we need high precision scattering amplitudes in Quantum Chromodynamics and the Standard Model, to reduce the theoretical uncertainty. The precise scattering amplitude computation suffers from problems of the large number of loop Feynman diagrams and difficult integrations for each loop diagram. This paper aims at developing a new method of reducing loop integrals to the minimal set of integrals, i.e., master integrals (MIs).

Traditionally, integral reduction can be achieved by applying integration-by-parts (IBP) identities [1] and considering the other symmetries of loop diagrams. However, given a two-loop or higher-loop integral, it is difficult to find a particular IBP identity which reduce it to MIs without introducing unwanted terms. There are several implements of IBPs generating codes AIR [2], FIRE [3–5] and Reduze [6, 7], based on Laporta algorithm [8], or LiteRed [9], based on a heuristic search of the symbolic IBP reductions. For multi-loop diagrams with high multiplicities or many mass scales, it may take a lot of time and computer RAM to finish the integral reduction. There are also several new approaches for integral reduction, based on the study of the Lie algebra structure of IBPs [10], Syzygy computation [11, 12], reductions over finite fields [13], and differential geometry [14]. Besides, the number of master integrals can be determined by the critical points of polynomials [15].

We present a new method of integral reduction, for a class of multi-loop diagrams, based on unitarity [16–33] and the analysis of *algebraic curves* [34–36]. We show that for a D-dimensional L-loop diagram, if the unitarity cut solution V is an irreducible algebraic curve, then the on-shell IBPs of this diagram correspond to *exact meromorphic 1-forms* on V. For an algebraic curve, it is very easy to find the exact meromorphic 1-forms, based on algebraic geometry. Hence for this class of diagrams, we can derive the on-shell part of IBPs very efficiently from our method.

Schematically, an IBP relation,

$$\int \frac{d^D l_1}{(2\pi)^D} \cdots \frac{d^D l_L}{(2\pi)^D} \frac{\partial}{\partial l_i^\mu} \frac{v_i^\mu}{D_1^{\alpha_1} \ldots D_k^{\alpha_k}} = 0 \tag{1.1}$$

on the unitarity cut $V : D_1 = \ldots = D_k = 0$ becomes contour integral relations [26–33],

$$\oint \omega = 0, \tag{1.2}$$

where the integrals are along combinations of non-trivial cycles of V, contours surrounding singular points of V and poles of ω. If V is an algebraic curve, then the contours are one-dimensional. Furthermore, if V is irreducible, then V has a complex structure and ω is a meromorphic 1-form [34]. In this case, (1.2) holds for all contours, so it implies the ω is an exact form,

$$\omega = dF, \tag{1.3}$$

where F is a meromorphic function on V. So the on-shell part of IBP relations for this diagram correspond to exact meromorphic 1-forms. Mathematically, it is very easy to find exact meromorphic 1-forms on an algebraic curve, so we can quickly get the on-shell IBPs for this diagram.

In this paper, we show several two-loop examples with internal masses for our new method. Multi-loop integrals with internal masses appear frequently in QCD/SM scattering amplitudes, and are bottlenecks for integral reduction or evaluation. We use these complicated cases to show the power of our method:

1. $D = 4$ planar double box with internal massive legs. The unitarity cut for this diagram is an elliptic curve. The maximal unitarity structure of the symmetric double box, with internal massive legs, was studied in [32]. Here we derive the integral reduction for the general cases, based on the analysis of differential forms on an elliptic curve. We also reduce integrals with doubled propagators based on algebraic curves, which were not considered in [32].

2. $D = 2$ sunset diagram. The unitarity cut for this diagram is again an elliptic curve. We derive the analytic integral reduction based on the analysis of elliptic curves.

3. $D = 4$ non-planar crossed box with internal massive legs. The unitarity cut for this diagram is a genus-3 hyperelliptic curve. The unitarity cut is more complicated than the planar two-loop counterparts, however, our method also works for this case. We get the analytic integral reduction from the analysis of the hyperelliptic curve.

In these examples, we get all the on-shell IBPs analytically. The algorithm is realized by a Mathematica code containing algebraic geometry tools. For each diagram, the analytic integral reduction is extremely fast, which has the time order of minutes.

We have the following remarks,

- Although the mathematic objects are elliptic or hyperelliptic, we do not need the explicit form of elliptic/hyperelliptic functions, or elliptic/hyperelliptic integrals. Only the differential relations for elliptic and hyperelliptic functions are needed. These relations involve rational coefficients only and are easy to find.

- The method presented in this paper is different from the maximal unitarity method. For the maximal unitarity method, we need to perform contour integrals to extract the master integral coefficients. Our method use the integrand reduction [37–40] via Gröbner basis [40–46] first, to reduce the loop amplitude to an integrand basis. Then we use the knowledge of algebraic curves, to reduce the integrand basis further to master integrals. In this way, we avoid the explicit elliptic or hyperelliptic integral computations.

- In this paper we just consider the integrand reduction and IBP on the maximal cut level. In order to get the complete integrand reduction and then to reduce all terms to master integrals, the complete set of IBPs is needed.

This paper is organized as follows: In section 2, we present our method based on algebraic curves. In section 3 and 4, the double box diagram (elliptic) and sunset diagram (elliptic) with internal masses will be explicitly presented. In section 5, we consider the integral reduction for the massive nonplanar box diagram (hyperelliptic). The rudiments of the knowledge of algebraic curves are included in the appendix.

2 Integral reduction via the analysis of algebraic curves

Generically, for a quantum field theory, the L-loop amplitude can be written as [16, 17],

$$A_n^{L\text{-loop}} = \sum_k c_k I_k + \text{rational terms}, \qquad (2.1)$$

The set $\{I_k\}$ is called the master integral (MI) basis whose elements are independent loop integrals. In practice, for amplitudes with multiple loops, high multiplicities or several mass scales, it is quite difficult to determine the set of master integral or reduce a generic integral,

$$\int \frac{d^D l_1}{(2\pi)^{D/2}} \cdots \frac{d^D l_L}{(2\pi)^{D/2}} \frac{N(l_1, \ldots l_L)}{D_1^{\alpha_1} \ldots D_k^{\alpha_k}}, \qquad (2.2)$$

to the linear combination of master integrals.

Traditionally, the integral reduction is done by using IBP identities [1],

$$\int \frac{d^D l_1}{(2\pi)^D} \cdots \frac{d^D l_L}{(2\pi)^D} \frac{\partial}{\partial l_i^\mu} \frac{v_i^\mu}{D_1^{\alpha_1} \ldots D_k^{\alpha_k}} = 0, \qquad (2.3)$$

if there is no boundary term. In general, it is difficult to find the IBP relations for a multi-loop integral reduction.

We present a new way of integral reduction, based on maximal unitarity method and algebraic curves. Given a Feynman integral with k propagators, maximal unitarity method split (2.1) as [18–33] ,

$$\text{Int} = \sum_i c_i I_i + \big(\text{integrals with fewer-than-k propagators}\big) + \text{rational terms} \qquad (2.4)$$

where the first sum is over the master integral with exact k propagators.

The condition the all internal legs are on-shell, is called the maximal unitarity cut,

$$V: \quad D_1 = \ldots = D_k = 0, \qquad (2.5)$$

and the solution set for this equation system is an *algebraic variety* V. V can be a set of discrete points, algebraic curves or surfaces. (See [47, 48] for the detailed mathematical study of multi-loop unitarity cut solutions.) Maximal unitarity replaces the original integral with contour integrals [26–33], schematically,

$$\int \frac{d^D l_1}{(2\pi)^D} \cdots \frac{d^D l_L}{(2\pi)^D} \frac{N(l_1, \ldots l_L)}{D_1^{\alpha_1} \ldots D_k^{\alpha_k}} \to \oint \frac{d^D l_1}{(2\pi)^D} \cdots \frac{d^D l_L}{(2\pi)^D} \frac{N(l_1, \ldots l_L)}{D_1^{\alpha_1} \ldots D_k^{\alpha_k}}$$
$$= \sum_j w_j \oint_{\mathcal{C}_j} \omega \qquad (2.6)$$

where ω is a differential form on V, and contours c_j's are around the poles of ω and also the *nontrivial cycles* of V [30, 32]. w_j are weights of these contours. In particular, to extract the coefficients c_i in (2.1), we can find a special set of weights $w_j^{\{i\}}$ [26–32] such that,

$$c_i = \sum_j w_j^{\{i\}} \oint_{\mathcal{C}_j} \omega \qquad (2.7)$$

For example, the $4D$ two-loop massless double box diagram contains 7 propagators. The maximal cut is a reducible variety with 6 components [26], each of which is a Riemann sphere. The contours are around the intersecting points of these Riemann spheres, which are singular points of this variety, and also around the poles of ω. For the $4D$ two-loop double box with massive internal legs, the maximal cut gives one irreducible variety, which is an elliptic curve [32]. There is no singular point on this variety, so the contours are around the poles of ω and also the *two fundamental cycles* on the elliptic curve.

Our observation is that if a differential form ω on V is integrated to zero, around all singular points on V, poles of ω and non-trivial cycles of V.

$$\oint_{\mathcal{C}_j} \omega = 0, \quad \forall j \qquad (2.8)$$

then from (2.7) and (2.4), the integral corresponding to ω can be reduced to integrals with fewer propagators. Since from the knowledge of algebraic geometry, it is easy to find

such ω's satisfying (2.8), we propose a new multi-loop integral reduction method from this viewpoint.

In this paper, we focus on the cases for which the number of propagators equals $DL-1$ and the maximal unitarity cut gives one irreducible variety. In such a case, the cut solution V is a smooth *algebraic curve* with well defined complex structure. The condition (2.8) implies that ω is an exact meromorphic form on V, since the integral

$$F(P) = \int_O^P \omega, \quad \forall P \in V \tag{2.9}$$

is independent of the path and $dF = \omega$. Then from the study of meromorphic functions on V, which is a well-known branch of algebraic geometry, we can list generators for F and then derive all forms which satisfy (2.8).

Explicitly, for this class of diagram, we found that the scalar integral on the cut becomes a holomorphic form on V.

$$\int \frac{d^D l_1}{(2\pi)^D} \cdots \frac{d^D l_L}{(2\pi)^D} \frac{1}{D_1 \dots D_k} \bigg|_{\text{cut}} = \oint \Omega \tag{2.10}$$

where the 1-form Ω is globally holomorphic (without poles) on V. On the cut, the components of l_i's become meromorphic functions. We can show that these functions generate all meromorphic functions on V. Let $F(l_1, \dots l_L)$ be a polynomial in the components of loop momenta, then take the derivative of F,

$$dF = f\Omega. \tag{2.11}$$

The resulting $f\Omega$ is an exact meromorphic 1-form. From the analysis above, we get that,

$$\int \frac{d^D l_1}{(2\pi)^D} \cdots \frac{d^D l_L}{(2\pi)^D} \frac{f}{D_1 \dots D_k} = 0 + (\text{integrals with fewer propagators}), \tag{2.12}$$

so we obtain an integral reduction relation. For the explicit examples in this paper, we can show that this method provides all the on-shell part of integral reduction relations.

In practice, our algorithm can be presented as,

1. Use integrand reduction method via Gröbner basis [41, 42] to rewrite the loop scattering amplitude as the form of *integrand basis*. The coefficients of integrand basis can be determined by fusing tree amplitudes or polynomial division of the Feynman integrand.

2. Calculate the maximal cut of the scalar integral to determine the holomorphic form Ω as (2.10).

3. Calculate the exterior derivatives of all polynomial F's. In practice, it is sufficient to consider the linear F's and then use the chain rule. Then we get all the on-shell IBP relations as (2.11).

4. Use the obtained integral reduction relations to reduce the integrand basis to master integrals.
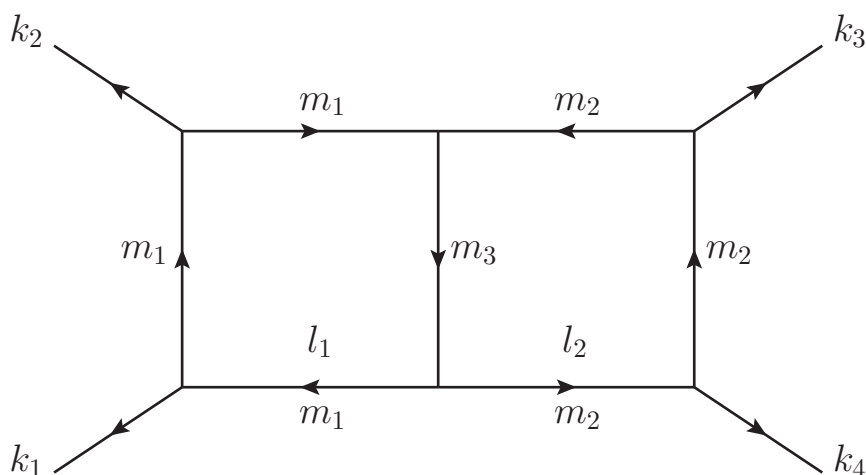
Figure 1. Planar double box diagram with 3 internal mass scales

If the integrand contains doubled-propagator integrals, the algorithm will be slightly different. We need to solve a polynomial Diophantine equation first, and the procedure will be shown in the next section.

Note that our algorithm is different from the traditional maximal unitarity. Usually, maximal unitarity method needs the explicit contour integration to extract the master integral coefficients. However, our algorithm does not require the explicit contour integration, and the explicit form of elliptic/hyperelliptic integral is not needed. The residue computations to find the holomorphic form Ω and the derivative computations (2.11) are much simpler than the contour integrals.

3   Elliptic example: double box with internal masses

The method explained in the previous section can be used for integral reduction for various topologies, for instance, the double-box (figure 1) with three different masses for the internal propagators. The maximal unitarity of the massless double box was discussed in [26]. Then, maximal unitarity structures for double box with $1 \sim 4$ massive external legs were studied in [27, 29]. In these cases, the unitarity cuts provide reducible curves.

On the other hand, the unitarity cut of double box with six massive external legs [30] or all massive internal legs provides irreducible curves. The integral reduction for symmetric double box diagram with internal masses, was discussed in [32], via maximal unitarity and the analysis of elliptic functions. Here we show the integral reduction for a more generic double box diagram with 3 internal mass scales, based on our new method, without using elliptic functions/integrals explicitly.

3.1 Maximal unitarity

The denominators for double box diagrams are

$$D_1 = l_1^2 - m_1^2\,, \qquad D_2 = (l_1 - k_1)^2 - m_1^2\,, \qquad D_3 = (l_1 - k_1 - k_2)^2 - m_1^2\,,$$
$$D_4 = l_2^2 - m_2^2\,, \qquad D_5 = (l_2 - k_4)^2 - m_2^2\,, \qquad D_6 = (l_2 - k_3 - k_4)^2 - m_2^2\,, \qquad (3.1)$$
$$D_7 = (l_1 + l_2)^2 - m_3^2\,.$$

We parametrize the loop momenta as,

$$l_1^\mu = \alpha_1 k_1^\mu + \alpha_2 k_2^\mu + \alpha_3 \frac{s}{2} \frac{\langle 1| \gamma^\mu |2]}{\langle 14 \rangle [42]} + \alpha_4 \frac{s}{2} \frac{\langle 2| \gamma^\mu |1]}{\langle 24 \rangle [41]}\,,$$
$$l_2^\mu = \beta_1 k_3^\mu + \beta_2 k_4^\mu + \beta_3 \frac{s}{2} \frac{\langle 3| \gamma^\mu |4]}{\langle 31 \rangle [14]} + \beta_4 \frac{s}{2} \frac{\langle 4| \gamma^\mu |3]}{\langle 41 \rangle [13]}\,, \qquad (3.2)$$

and the Jacobian for this parameterization is,

$$J_1 = \det_{\mu,i} \frac{\partial l_1^\mu}{\partial \alpha_i} = \frac{\mathrm{i} s^4}{4t(s+t)}\,, \qquad J_2 = \det_{\mu,i} \frac{\partial l_2^\mu}{\partial \beta_i} = \frac{\mathrm{i} s^4}{4t(s+t)}\,. \qquad (3.3)$$

The solutions for the maximal unitarity cut,

$$D_1 = D_2 = \ldots = D_7 = 0\,. \qquad (3.4)$$

defines an elliptic curve. To see this, we first solve for the variables α_1, α_2, α_3, β_1, β_2 and β_3 in terms of α_4 and β_4,

$$\alpha_1 = 1\,, \qquad \alpha_2 = 0\,, \qquad \alpha_3 = \frac{m_1^2 t(s+t)}{\alpha_4 s^3}\,,$$
$$\beta_1 = 0\,, \qquad \beta_2 = 1\,, \qquad \beta_3 = \frac{m_2^2 t(s+t)}{\beta_4 s^3}\,, \qquad (3.5)$$

Then the remaining one equation relates α_4 and β_4,

$$K(\alpha_4, \beta_4) = A(\alpha_4)\beta_4^2 + B(\alpha_4)\beta_4 + C(\alpha_4) = 0\,, \qquad (3.6)$$

Here $A(\alpha_4)$, $B(\alpha_4)$ and $C(\alpha_4)$ are quadratic polynomials of α_4, whose coefficients depend on kinematic variables. Formally, β_4 depends on α_4 as,

$$\beta_4 = \frac{-B(\alpha_4) \pm \sqrt{\Delta(\alpha_4)}}{2A(\alpha_4)}\,, \quad \Delta = B^2 - 4AC, \qquad (3.7)$$

where Δ is a quartic polynomial in α_4 with *four distinct roots*, for generic kinematics with internal masses. Hence the maximal unitarity cut defines an elliptic curve, i.e., algebraic curve with genus one,

$$\mathcal{C} : \eta^2 = \Delta(\alpha_4)\,, \qquad (3.8)$$

(See the appendix for the basis introduction to elliptic curves.) The choice of keeping α_4 and β_4 and eliminating other variables is purely arbitrary.

On the cut, by a short calculation, the scalar double box integral,

$$I = \int \frac{d^4 l_1}{(2\pi)^4} \frac{d^4 l_2}{(2\pi)^4} \frac{1}{D_1 \ldots D_7} \,, \tag{3.9}$$

has the following structure:

$$I|_{7-cut} = \frac{s^2 t}{16} \oint \frac{d\alpha_4}{\sqrt{\Delta}} \tag{3.10}$$

where the overall factor is not important for the following discussion.

As [32], it is remarkable that $\frac{d\alpha_4}{\sqrt{\Delta}}$ is the only *holomorphic one-form* associated with the elliptic curve. On the cut, the loop-momentum components α_i, β_i become elliptic functions. So we may study the explicit form of these functions, calculate the elliptic integrals and perform the integral reduction, in a procedure of [32]. However, in this paper, we propose a different procedure: (1) reduce the integrand based on Gröbner basis [41, 42] (2) reduce the integrand basis to master integrals by the study of differential forms on the elliptic curve. The advantage of this approach is that the whole computation is very simple: no explicit elliptic parameterization or elliptic integral is needed. The new process can also be easily automated on computer algebra systems.

3.2 Integral reduction

We now focus on the double box integral with numerator N,

$$I[N] = \int \frac{d^4 l_1}{(2\pi)^4} \frac{d^4 l_2}{(2\pi)^4} \frac{N}{D_1 \ldots D_7} \,, \tag{3.11}$$

Integrand reduction method via Gröbner basis method [41, 42] determines that the integrand basis contains 32 terms. In terms of (3.2), the basis can be presented as,

$$\mathcal{B} = \{\alpha_3^4 \beta_3, \alpha_4 \beta_4^4, \alpha_4 \beta_3^4, \alpha_4^4 \beta_3, \beta_3^4, \beta_3^4, \alpha_3^3 \beta_3, \alpha_3^4, \alpha_4 \beta_4^3, \alpha_4 \beta_3^3, \alpha_3^3 \beta_3, \alpha_4^4, \beta_4^3, \beta_3^3, \alpha_3^2 \beta_3, \alpha_3^3,$$
$$\alpha_4 \beta_4^2, \alpha_4 \beta_3^2, \alpha_4^2 \beta_3, \alpha_4^3, \beta_4^2, \beta_3^2, \alpha_3 \beta_3, \alpha_3^2, \alpha_4 \beta_4, \alpha_4 \beta_3, \alpha_4^2, \beta_4, \beta_3, \alpha_3, \alpha_4, 1\} \tag{3.12}$$

On the cut, the integral becomes a meromorphic one-form,

$$I[N]|_{\text{cut}} \propto \oint \frac{d\alpha_4}{\eta} N(\alpha_3, \alpha_4, \beta_3, \beta_4) \tag{3.13}$$

where N is a polynomial in α_3, α_4, β_3 and β_4, and therefore also an elliptic function. We now perform the integral reduction, following the strategy as in the previous section. The task is to find *exact meromorphic one-forms* ω on this elliptic curves. If two integrals on the cut, differ by the contour integrals of such an ω, then

$$I[N_1] - I[N_2]|_{\text{cut}} = \oint \omega = 0 \tag{3.14}$$

where the second equality holds for all contours, i.e., two fundamental cycles and small contours around the poles, because ω is exact. Then the integral reduction between $I[N_1]$ and $I[N_2]$ is achieved at the level of double box diagram,

$$I[N_1] - I[N_2] = 0 + (\text{integrals with} < 7 \text{ propagators}) \tag{3.15}$$

Note the α_4 and β_4 generate *all* elliptic functions on this elliptic curve, as shown in the appendix, (A.5).

In practice, we find that to find such ω's, it is sufficient to consider the exterior derivatives of polynomials in α_3, α_4, β_3 and β_4,

$$dF(\alpha_3, \alpha_4, \beta_3, \beta_4) = \frac{\partial F}{\partial \alpha_3} d\alpha_3 + \frac{\partial F}{\partial \alpha_4} d\alpha_4 + \frac{\partial F}{\partial \beta_3} d\beta_3 + \frac{\partial F}{\partial \beta_4} d\beta_4 \equiv f \frac{d\alpha_4}{\eta} \qquad (3.16)$$

So we need to find the one forms $\{d\alpha_3, d\alpha_4, d\beta_3, d\beta_4\}$ and then use the chain rule to generate integral reduction relations. We can start by calculating $d\alpha_4$ in terms of the holomorphic one-form,

$$d\alpha_4 = \eta \frac{d\alpha_4}{\eta} = (2A(\alpha_4)\beta_4 + B(\alpha_4))\frac{d\alpha_4}{\eta}, \qquad (3.17)$$

where we used the definition $\eta = \sqrt{\Delta}$ and (3.7) to rewrite η in function of β_4. The purpose of this step is to get the polynomial form of f.

We can now easily find $d\alpha_3$,

$$d\alpha_3 = d\left(\frac{\lambda_1}{\alpha_4}\right) = -\lambda_1 \frac{1}{\alpha_4^2} d\alpha_4 = -\frac{\alpha_3^2}{\lambda_1} d\alpha_4, \quad \lambda_1 \equiv \frac{m_1^2 t(s+t)}{s^3} \qquad (3.18)$$

the constant λ_1 is the product of $\alpha_3\alpha_4$ on the cut. To generate the remaining 1-forms, we again use the form of elliptic curve. Recall that,

$$K(\alpha_4, \beta_4) = A(\alpha_4)\beta_4^2 + B(\alpha_4)\beta_4 + C(\alpha_4) = 0. \qquad (3.19)$$

The identity $dK = 0$ reads,

$$d\beta_4 = -\left(A'(\alpha_4)\beta_4^2 + B'(\alpha_4)\beta_4 + C'(\alpha_4)\right)\frac{d\alpha_4}{\eta}. \qquad (3.20)$$

Finally we can easily calculate $d\beta_3$,

$$d\beta_3 = d\left(\frac{\lambda_2}{\beta_4}\right) = -\lambda_2 \frac{1}{\beta_4^2} d\beta_4 = -\frac{\beta_3^2}{\lambda_2} d\beta_4, \quad \lambda_2 \equiv \frac{m_2^2 t(s+t)}{s^3} \qquad (3.21)$$

Then using the chain rule, we get all the on-shell IBPs. For example, from (3.16), we analytically obtain this relation,

$$
\begin{aligned}
I_{\text{dbox}}[\alpha_4^3] = \frac{1}{2s^4(4m_2^2 - s)}\bigg(& 3s^3 \left(m_1^2 s - m_2^2 s - m_3^2 s - 4m_2^2 t + st\right) I_{\text{dbox}}[\alpha_4^2] \\
& + s(4m_1^2 s^2 t - 2m_2^2 s^2 t - 2m_3^2 s^2 t + m_1^4 s^2 - 2m_2^2 m_1^2 s^2 - 2m_3^2 m_1^2 s^2 + m_2^4 s^2 + m_3^4 s^2 \\
& - 2m_2^2 m_3^2 s^2 + 2m_1^2 st^2 - 4m_2^2 st^2 - 8m_2^2 m_1^2 st - 8m_2^2 m_1^2 t^2 + s^2 t^2) I_{\text{dbox}}[\alpha_4] \\
& + m_1^2 t(s+t) \left(m_1^2 s - m_2^2 s - m_3^2 s - 4m_2^2 t + st\right) I_{\text{dbox}}[1] \bigg) + \dots \qquad (3.22)
\end{aligned}
$$

where ... stands for integrals with fewer than 7 propagators. Considering all polynomials whose exterior derivative satisfy the renormalizability conditions, we obtain 23 integral relations. Furthermore, considering Levi-Civita insertions which integrate to zero,

$$\epsilon(l_2, k_1, k_2, k_3)\, l_2 \cdot k_1, \quad \epsilon(l_2, k_1, k_2, k_3)\, l_1 \cdot k_4, \quad \epsilon(l_1, l_2, k_1, k_2), \quad \epsilon(l_1, l_2, k_1, k_3). \qquad (3.23)$$

– 9 –

we get 4 more integral relations. So the total number of MIs is,

$$\#\mathrm{MI}_{\mathrm{dbox}} = 32 - 23 - 4 = 5 \tag{3.24}$$

and explicitly the MIs can be chosen as,

$$\mathrm{MI}_{\mathrm{dbox}} = \left\{ I_{\mathrm{dbox}}[\alpha_4\beta_3], I_{\mathrm{dbox}}[\alpha_4^2], I_{\mathrm{dbox}}[\alpha_4], I_{\mathrm{dbox}}[\beta_3], I_{\mathrm{dbox}}[1] \right\} . \tag{3.25}$$

or in the conventional choice with $X \equiv (l_1 + k_4)^2/2$ and $Y \equiv (l_2 + k_1)^2/2$,

$$\mathrm{MI}_{\mathrm{dbox}} = \left\{ I_{\mathrm{dbox}}[XY], I_{\mathrm{dbox}}[X^2], I_{\mathrm{dbox}}[X], I_{\mathrm{dbox}}[Y], I_{\mathrm{dbox}}[1] \right\} . \tag{3.26}$$

and for instance, the integral reduction in this basis becomes,

$$\begin{aligned}
I_{\mathrm{dbox}}[X^3] =& \frac{1}{16s\left(4m_2^2 - s\right)} \big(I_{\mathrm{dbox}}[1] \left(8m_1^6 m_2^2 s - m_1^4 \left(m_2^2 \left(s^2 + 4st + 16t^2 \right) + m_3^2 s^2 \right) + \right. \\
& + m_1^2 s \left(-m_2^4 s + 2m_2^2 \left(m_3^2 s + t(s + 4t) \right) + m_3^2 \left(2t(s + 2t) - m_3^2 s \right) \right) + \\
& \left. - s^2 t \left(m_2^4 + m_2^2 \left(t - 2m_3^2 \right) + m_3^2 \left(m_3^2 + t \right) \right) \right) + 2 I_{\mathrm{dbox}}[X] \left(m_1^4 s \left(s - 24m_2^2 \right) + \right. \\
& + 2m_1^2 \left(2m_2^2 \left(s^2 - 2st + 4t^2 \right) + s \left(2m_3^2 s - t(s + 2t) \right) \right) \\
& + s \left(m_2^4 s - 2m_2^2 \left(m_3^2 s + 2t(t - s) \right) + + s \left(m_3^4 + 4m_3^2 t + t^2 \right) \right) \right) \\
& - 12 I_{\mathrm{dbox}}[X^2] s \left(m_1^2 \left(s - 8m_2^2 \right) + m_2^2 (s - 4t) + s \left(m_3^2 + t \right) \right) \big) \\
& + \dots \tag{3.27}
\end{aligned}$$

The whole computation takes about 120 seconds with our Mathematica code. The relations are numerically verified by FIRE [3, 4].

3.3 Reduction of the double-propagator integrals

One issue not discussed in [32] is the reduction of integral with internal mass and *doubled propagators*. For the double box diagram, the doubled-propagator integrand on the cut also becomes a meromorphic 1-form, so we may carry out the maximal unitarity analysis as that in [32]. However, in this section, we show that, our new method is more efficient for reducing these integrals.

Consider the diagram in figure 1 with the middle propagator doubled,

$$I_{\mathrm{dbox},2} = \int \frac{d^4 l_1}{(2\pi)^4} \frac{d^4 l_2}{(2\pi)^4} \frac{1}{D_1 D_2 D_3 D_4 D_5 D_6 D_7^2} , \tag{3.28}$$

on the cut, by the degenerate residue computation with *transformation law* or *Bezoutian matrix computation* [49, 50], we have,

$$I_{\mathrm{dbox},2}|_{7-cut} = -\frac{s^6 t^2}{16} \oint \frac{\alpha_4 B(a_4) d\alpha_4}{\Delta^{3/2}}. \tag{3.29}$$

Unlike the one-forms in the previous subsection, here the one-form have the denominator $\Delta^{3/2}$. It implies that we need to find exact 1-forms like $d(F/\Delta^{1/2})$, where F is a polynomial in the loop-momenta components.

Note that $\Delta(a_4)$ has four distinct roots, hence $\Delta(\alpha_4)$ and $\Delta'(\alpha_4)$ have no common root. By Bézout's identity,

$$\langle \Delta(a_4), \Delta'(a_4) \rangle = \langle 1 \rangle \tag{3.30}$$

and the polynomial Diophantine equation

$$f_1(\alpha_4)\Delta(\alpha_4) + f_2(\alpha_4)\Delta'(\alpha_4) = \alpha_4 B(\alpha_4) \tag{3.31}$$

has solutions. Such polynomials f_1 and f_2 can be explicitly found by Euclidean division or Gröbner basis method. The exterior derivative,

$$d\left(\frac{-2f_2}{\Delta^{1/2}}\right) = \frac{f_2\Delta'}{\Delta^{3/2}}d\alpha_4 - 2\frac{f_2'}{\Delta^{1/2}}d\alpha_4 \tag{3.32}$$

determines that,

$$I_{\text{dbox},2}|_{7-cut} = -\frac{s^6 t^2}{16}\oint \frac{(f_1 + 2f_2')d\alpha_4}{\Delta^{1/2}}. \tag{3.33}$$

after integrating out the exact form. Now the term $\Delta^{3/2}$ is removed and we can reduce this integral using the result from the previous subsection. In practice, we find a solution such that $f_1 + 2f_2'$ is a quadratic polynomial in α_4, so at the level of the double box,

$$I_{\text{dbox},2} = c_0 I_{\text{dbox}}[1] + c_1 I_{\text{dbox}}[X] + c_2 I_{\text{dbox}}[X^2] + \ldots \tag{3.34}$$

The three coefficients c_0, c_1 and c_2 are analytically found by our method and numerically verified by FIRE [3, 4].

4 Elliptic example: sunset diagram

The sunset diagram is a two-loop diagram which attracts a lot of research interests [51–73]. The sunset diagram with 3 different masses is the simplest loop diagram which cannot be expresses in multiple polylogarithms.

We use our method to study the integral reduction of the sunset diagram (figure 2) in two dimensional space-time. In this example, we assume that all internal propagators are massive.

Let p be the external momentum, $p^2 = m^2$. We can parametrize the loop momenta using a variant of Van-Neerven Vermaseren basis [74]. Define two null vectors e_1 and e_2 such that $e_1^2 = 0$, $e_2^2 = 0$ and $e_1 \cdot e_2 = p^2$. The Gram matrix of $\{e_1, e_2\}$ is,

$$G = \begin{pmatrix} 0 & m^2 \\ m^2 & 0 \end{pmatrix} \tag{4.1}$$

In this basis we expand p as,

$$p = e_1 + \frac{e_2}{2}, \tag{4.2}$$

and define the auxiliary vector ω,

$$\omega = e_1 - \frac{e_2}{2}. \tag{4.3}$$
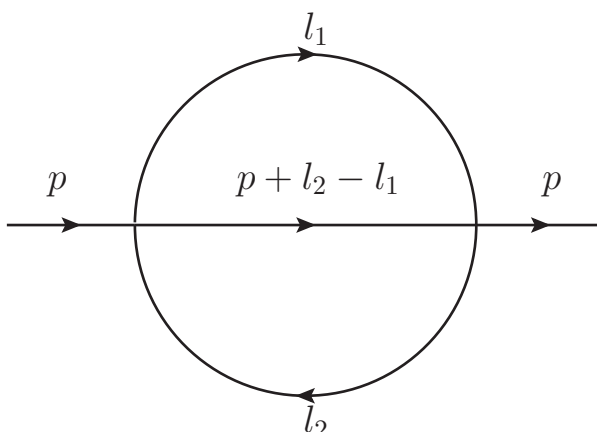
– 11 –

Figure 2. Sunset diagram

Hence $p \cdot \omega = 0$. The two loop momenta can be then generally parametrized as

$$
\begin{aligned}
l_1 &= \alpha_1 e_1 + \alpha_2 e_2 \,, \\
l_2 &= \beta_1 e_1 + \beta_2 e_2 \,,
\end{aligned}
\tag{4.4}
$$

On-shell equations are $D_1 = D_2 = D_3 = 0$, where D_i represent the inverse propagators,

$$
D_1 = l_1^2 - m_1^2 \,, \qquad D_2 = (p + l_2 - l_1)^2 - m_2^2 \,, \qquad D_3 = l_2^2 - m_3^2 \,.
\tag{4.5}
$$

The on-shell solution can be formally expressed as,

$$
\alpha_1 = \frac{m_1^2}{2\alpha_2 p^2} \,, \qquad \beta_1 = \frac{m_3^2}{2\beta_2 p^2} \,, \qquad \beta_2 = \frac{-B(\alpha_2) \pm \sqrt{\Delta(\alpha_2)}}{2A(\alpha_2)} \,.
\tag{4.6}
$$

where again α_2 and β_2 satisfy the equation of an elliptic curve $A(\alpha_2)\beta_2^2 + B(\alpha_2)\beta_2 + C(\alpha_2) = 0$. The discriminant is $\Delta = B^2 - 4AC$.

The sunset integral, on the triple cut, becomes contour integrals of holomorphic 1-forms

$$
I|_{3-cut} \propto \oint \frac{d\alpha_4}{\eta}, \quad \eta \equiv \sqrt{\Delta(\alpha_2)}
\tag{4.7}
$$

The integrand basis for the sunset diagram, obtained from Gröbner basis method [14, 42], contains 12 terms.

$$
\left\{ \alpha_1^2, \alpha_2^2, \alpha_1\beta_1, \beta_1^2, \alpha_2\beta_1, \alpha_2\beta_2, \beta_2^2, \alpha_1, \alpha_2, \beta_1, \beta_2, 1 \right\}
\tag{4.8}
$$

We now consider the integral reduction for figure 2, since the structure is elliptic we follow the same strategy as the double box case. As in the double box case, we find the one forms $\{d\alpha_1, d\alpha_2, d\beta_1, d\beta_2\}$ and then use the chain rule to generate all the IBP relations. We start by calculating $d\alpha_2$,

$$
d\alpha_2 = \frac{\eta}{\eta} d\alpha_2 = (2A(\alpha_2)\beta_2 + B(\alpha_2)) \frac{d\alpha_2}{\eta} \,,
\tag{4.9}
$$

we have used (4.6) to rewrite η in function of β_2. We can now easily find $d\alpha_1$,

$$d\alpha_1 = d\left(\frac{\lambda_1}{\alpha_2}\right) = -\lambda_1 \frac{1}{\alpha_2^2} d\alpha_2 = -\frac{\alpha_1^2}{\lambda_1} d\alpha_2, \quad \lambda_1 \equiv \frac{m_1^2}{2m^2} \tag{4.10}$$

Then,

$$d\beta_2 = -\left(A'(\alpha_2)\beta_2^2 + B'(\alpha_2)\beta_2 + C'(\alpha_2)\right)\frac{d\alpha_2}{\eta}. \tag{4.11}$$

Again we can easily calculate $d\beta_1$

$$d\beta_1 = d\left(\frac{\lambda_2}{\beta_2}\right) = -\lambda_2 \frac{1}{\beta_2^2} d\beta_2 = -\frac{\beta_1^2}{\lambda_2} d\beta_2, \quad \lambda_2 \equiv \frac{m_3^2}{2m^2} \tag{4.12}$$

To generate the 1-forms, given a function F which is a polynomial in α_1, α_2, β_1 and β_2, we can use

$$dF = \frac{\partial F}{\partial \alpha_1} d\alpha_1 + \frac{\partial F}{\partial \alpha_2} d\alpha_2 + \frac{\partial F}{\partial \beta_1} d\beta_1 + \frac{\partial F}{\partial \beta_2} d\beta_2 \tag{4.13}$$

to generate the on-shell part of IBPs. Furthermore, note that the Levi-Civita insertions

$$l_1 \cdot \omega, \quad l_2 \cdot \omega, \quad l_1 \cdot \omega \, l_1 \cdot p, \quad l_2 \cdot \omega \, l_1 \cdot p. \tag{4.14}$$

are integrated to zero. In total, we generate 4 IBPs and 4 independent Levi-Civita insertions integral relations. Hence, there are $12 - 4 - 4 = 4$ master integrals for the sunset diagram. Define that $X = l_1 \cdot p$ and $Y = l_2 \cdot p$, the four master integrals can be chosen as,

$$\mathrm{MI}_{\mathrm{sunset}} = \left\{ I_{\mathrm{sunset}}[1], I_{\mathrm{sunset}}[X], I_{\mathrm{sunset}}[X^2], I_{\mathrm{sunset}}[Y] \right\}. \tag{4.15}$$

For instance, the reduction reads,

$$\begin{aligned}
I_{\mathrm{sunset}}[XY] = {} & \frac{1}{4}\left(m^4 + m_1^2 m^2 - m_2^2 m^2 + m_3^2 m^2\right) I_{\mathrm{sunset}}[1] \\
& + \frac{1}{4}\left(-3m^2 - m_1^2 + m_2^2 - m_3^2\right) I_{\mathrm{sunset}}[X] \\
& + \frac{1}{2} I_{\mathrm{sunset}}[X^2] + \frac{1}{2}\left(m^2 + m_1^2\right) I_{\mathrm{sunset}}[Y] + \dots
\end{aligned} \tag{4.16}$$

where ... stands for integrals with fewer than 3 propagators.

Note that generically, D-dimensional sunset diagrams with 3 distinct masses have 4 master integral. The four master integrals can be chosen as (4.15) or the scalar integral and three doubled-propagator integrals. There is a subtlety that if $D = 2$, then the 4 master integrals are related by Schouten identities [70]. These identities are valid for $D < 3$, and at $D = 2$ they further reduce the number of master integrals from 4 to 2.

5   Hyperelliptic example: nonplanar crossed box with internal masses

We now proceed in studying the integral reduction of the massive nonplanar double box (figure 3). Unlike the previous examples, this diagram's maximal unitarity cut provides a genus-3 hyperelliptic curve [47, 48]. The structure of holomorphic/meromorphic forms
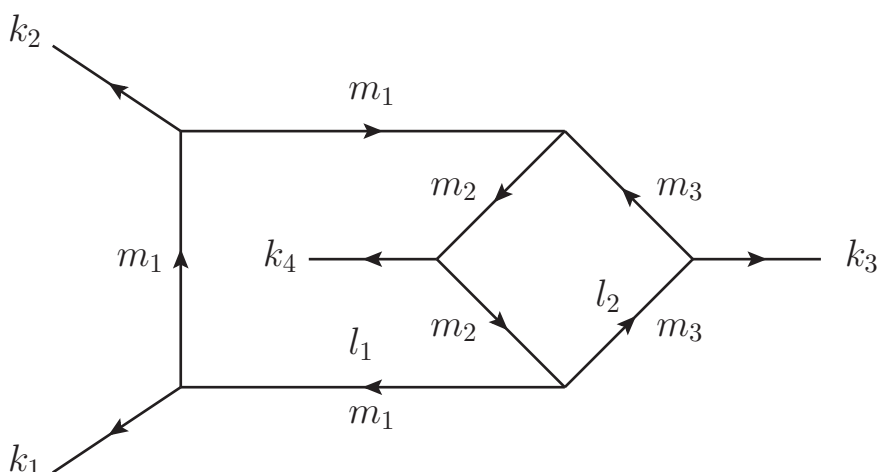
Figure 3. Nonplanar double box

on this curve is different from the elliptic case. However, our new approach for integral reduction works for this case as well.

To illustrate our method, we consider the two-loop crossed box diagrams with massless external legs and three internal mass scales $\{m_1, m_2, m_3\}$. Our method also works for other crossed box configurations with all massive internal legs.

5.1 Maximal unitarity and geometric properties

The denominators for the figure 3 are,

$$
\begin{aligned}
D_1 &= l_1^2 - m_1^2, & D_2 &= (l_1 - k_1)^2 - m_1^2, & D_3 &= (l_1 - k_1 - k_2)^2 - m_1^2, \\
D_4 &= l_2^2 - m_3^2, & D_5 &= (l_2 - k_3)^2 - m_3^2, & D_6 &= (l_1 - l_2 + k_4)^2 - m_2^2, \\
D_7 &= (l_1 + l_2)^2 - m_2^2.
\end{aligned}
\tag{5.1}
$$

The on-shell constrains are

$$
D_1 = \ldots = D_7 = 0,
\tag{5.2}
$$

We use the same loop momenta parametrization (3.2). Again, we first solve for α_1, α_2, α_3, β_1, β_2 and β_4 in terms of α_4 and β_3,

$$
\begin{aligned}
\alpha_1 &= 1, & \alpha_2 &= 0, & \alpha_3 &= \frac{m_1^2 t(s+t)}{\alpha_4 s^3}, \\
\beta_1 &= -\left(\alpha_4 + \alpha_3 + \frac{t}{s}\right), & \beta_2 &= 0, & \beta_4 &= \frac{(m_3^2) t(s+t)}{\beta_3 s^3}.
\end{aligned}
\tag{5.3}
$$

The rest two variables satisfy a polynomial equation,

$$
K(\alpha_4, \beta_3) = A(\alpha_4)\beta_3^2 + B(\alpha_4)\beta_3 + C(\alpha_4) = 0,
\tag{5.4}
$$

– 14 –

whose solution can be formally represented as,

$$\beta_3 = \frac{-B(\alpha_4) \pm \sqrt{\Delta(\alpha_4)}}{2A(\alpha_4)}, \quad \Delta \equiv B^2 - 4AC \tag{5.5}$$

Unlike the previous examples, $\Delta(\alpha_4)$ here is a degree-8 polynomial in α_4 with 8 distinct roots. Hence the unitarity cut of this diagram provides a genus-3 hyperelliptic curve. (See the appendix for the classification of complex algebraic curves). Note that not all genus-3 algebraic curves are hyperelliptic, but this one is because of (5.4).

Before the integral reduction, it is interesting to the see the geometric properties of this unitarity cut. Using (5.4) and the statements of appendix, we see that the function α_4 is a meromorphic function of degree 2 on the curve, i.e., it has two poles P_1, P_2 and two zeros Q_1, Q_2. Explicitly, we can check that Q_1 and Q_2 are distinct, therefore, in the language of divisors (A.7),

$$(\alpha_4) = Q_1 + Q_2 - P_1 - P_2 \,. \tag{5.6}$$

The divisor of α_3 is then

$$(\alpha_3) = P_1 + P_2 - Q_1 - Q_2 \,. \tag{5.7}$$

The divisor for the function β_3 and β_4 is more complicated. From (5.4), we determined that β_3 on the cut becomes a meromorphic functions of 4 simple poles. The divisor of β_3 is:

$$(\beta_3) = P_2 + Q_2 + W_1 + W_2 - P_1 - Q_1 - Z_1 - Z_2 \,. \tag{5.8}$$

We find that two poles of α_4 become a pole and a zero of β_3. Similarly, the two zeros of α_4 also become a pole and a zero of β_3. The divisor of β_4 is:

$$(\beta_4) = P_1 + Q_1 + Z_1 + Z_2 - P_2 - Q_2 - W_1 - W_2 \,. \tag{5.9}$$

In summary, there are 8 poles on this hyperelliptic curve from numerators insertions, namely P_1, P_2, Q_1, Q_2, Z_1, Z_2, W_1 and W_1.

5.2 Integral reduction

First, the integrand reduction via Gröbner basis [41, 42] determines that, the integrand basis contains 38 terms in the numerator,

$$\begin{aligned}
\{&\alpha_3^5\beta_3, \alpha_3^6, \alpha_4^5\beta_3, \alpha_4^6, \alpha_3^4\beta_3, \alpha_3^5, \alpha_4\beta_4^4, \alpha_4\beta_3^4, \alpha_4^4\beta_3, \alpha_4^5, \beta_4^4, \beta_3^4, \alpha_3^3\beta_3, \alpha_3^4, \alpha_4\beta_4^3, \\
&\alpha_4\beta_3^3, \alpha_4^3\beta_3, \alpha_4^4, \beta_4^3, \beta_3^3, \alpha_3^2\beta_3, \alpha_3^3, \alpha_4\beta_4^2, \alpha_4\beta_3^2, \alpha_4^2\beta_3, \alpha_4^3, \beta_4^2, \beta_3^2, \alpha_3\beta_3, \alpha_3^2, \\
&\alpha_4\beta_4, \alpha_4\beta_3, \alpha_4^2, \beta_4, \beta_3, \alpha_3, \alpha_4, 1\}
\end{aligned} \tag{5.10}$$

Then, consider the maximal cut for the scalar integral of this diagram. The residue computation gives,

$$I_{\mathrm{xbox}}[1]|_{7-cut} = \frac{s^3(s+t)}{16} \oint \frac{\alpha_4 d\alpha_4}{\sqrt{\Delta(\alpha_4)}} \,. \tag{5.11}$$

Note that unlike the elliptic case, on a genus-3 curve there are three holomorphic 1-forms from (A.13), (which have no pole on the hyperelliptic curve),

$$\frac{d\alpha_4}{\sqrt{\Delta(\alpha_4)}}, \quad \frac{\alpha_4 d\alpha_4}{\sqrt{\Delta(\alpha_4)}}, \quad \frac{\alpha_4^2 d\alpha_4}{\sqrt{\Delta(\alpha_4)}} \tag{5.12}$$

– 15 –

the scalar integral cut corresponds to the second one, while

$$I_{\text{xbox}}[\alpha_4]|_{7-cut} \propto \oint \frac{\alpha_4^2 d\alpha_4}{\sqrt{\Delta(\alpha_4)}}, \quad I_{\text{xbox}}[\alpha_3]|_{7-cut} \propto \oint \frac{d\alpha_4}{\sqrt{\Delta(\alpha_4)}}. \quad (5.13)$$

It is curious that for a crossed box integral with the numerator linear in l_1, the maximal cut always gives a holomorphic 1-form.

This hyperelliptic curve have 6 fundamental cycles and 8 poles as shown in the previous subsection. By global residue theorem, only 7 poles' residues are independent. Therefore we may perform maximal unitarity by computing integrals over $6+7 = 13$ contours. Since here we only have one unitarity cut solution, the number of master integers must be less than or equal 13. However, in the following discussion, for the purpose of the integral reduction, we use our new approach to find exact meromorphic forms instead of calculating these integrals explicitly.

Following what we did for elliptic cases, we would like to generate the IBP relations by exact meromorphic 1-forms on the hyperelliptic curve. Again, we calculate the differential forms $\{d\alpha_3, d\alpha_4, d\beta_3, d\beta_4\}$.

$$d\alpha_4 = \frac{\eta}{\eta} d\alpha_4 = (2A(\alpha_4)\beta_4 + B(\alpha_4)) \frac{d\alpha_4}{\eta} = (2A(\alpha_4)\beta_4 - B(\alpha_3)) \frac{\alpha_3}{\lambda_1} \frac{\alpha_4 \, d\alpha_4}{\eta}, \quad (5.14)$$

where we have used the usual definition $\eta \equiv \sqrt{\Delta}$. In the second equality, we used the on-shell identity,

$$\alpha_3 \alpha_4 = \lambda_1 \equiv \frac{m_1^2 t(s+t)}{s^3}, \quad (5.15)$$

to recover the form of the scalar integral cut (5.11). The step is not needed for the elliptic cases. Then,

$$d\alpha_3 = d\left(\frac{\lambda_1}{\alpha_4}\right) = -\lambda_1 \frac{1}{\alpha_4^2} d\alpha_4 = -\frac{\alpha_3^2}{\lambda_1} d\alpha_4, \quad (5.16)$$

where again we have used (5.3) to simplify our expression. The exterior derivatives for β_i are more complicated,

$$d\beta_3 = -\left(A'(\alpha_4)\beta_3^2 + B'(\alpha_4)\beta_3 + C'(\alpha_4)\right) \frac{\alpha_3}{\lambda_1} \frac{\alpha_4 d\alpha_4}{\eta}, \quad (5.17)$$

and,

$$d\beta_4 = d\left(\frac{\lambda_2}{\beta_3}\right) = -\lambda_2 \frac{1}{\beta_3^2} d\beta_3 = -\frac{\beta_4^2}{\lambda_2} d\beta_3, \quad \lambda_2 = \frac{m_3^2 t(s+t)}{s^3} \quad (5.18)$$

Given a polynomial function of $\{\alpha_i, \beta_i\}$, we can use the chain rule to generate the on-shell IBPs.

We also consider Levi-Civita insertions which are integrated to zero,

$$\begin{array}{ccc}
\epsilon(l_2, k_2, k_3, k_4)\, l_2 \cdot k_1, & \epsilon(l_2, k_2, k_3, k_4)\, l_1 \cdot k_4, & \epsilon(l_1, l_2, k_1, k_2), \\
\epsilon(l_1, l_2, k_1, k_3), & \epsilon(l_1, k_2, k_3, k_4), & \epsilon(l_2, k_2, k_3, k_4).
\end{array} \quad (5.19)$$

In total, we generate 25 on-shell IBPs and 6 Levi-Civita insertions identities. Hence there are $38 - 25 - 6 = 7$ MIs for the non-planar crossed box diagram with three internal mass scales. Define that $X = (l_1 + p_4)^2/2$ and $Y = (l_2 + p_1)^2/2$, and the MIs can be chosen as:

$$\left\{ I_{\text{xbox}}[X^3], I_{\text{xbox}}[Y^2], I_{\text{xbox}}[XY], I_{\text{xbox}}[X^2], I_{\text{xbox}}[X], I_{\text{xbox}}[Y], I_{\text{xbox}}[1] \right\}. \tag{5.20}$$

For this non-planar diagram, the analytic integral reduction relations are significantly more complicated. For example,

$$
\begin{aligned}
I_{\text{xbox}}\left[Y^3\right] =& \frac{I_{\text{xbox}}\left[X^3\right](28m_1^2 s + 2m_3^2 s - 7s^2 + 4m_3^2 t - 2m_2^2(s+2t))}{8(4m_1^2 - s)s} + \\
&+ \frac{3I_{\text{xbox}}\left[Y^2\right](4m_1^2(4m_3^2 - s - 2t) + s(-2m_2^2 - 2m_3^2 + s + 2t))}{32m_1^2 - 8s} + \\
&- \frac{I_{\text{xbox}}\left[XY\right](4m_1^2(s+2t) - s(6m_2^2 - 6m_3^2 + s + 2t))}{32m_1^2 - 8s} + \\
&- \frac{I_{\text{xbox}}\left[X^2\right](3m_1^2 - s + t)(28m_1^2 s + 2m_3^2 s - 7s^2 + 4m_3^2 t - 2m_2^2(s+2t))}{16(4m_1^2 - s)s} \\
&- \frac{1}{16(4m_1^2 - s)s}I_{\text{xbox}}\left[Y\right](4m_1^4(3s^2 + 2st + 4t^2) + s(-2m_2^4 s - 2m_3^4 s - st(3s + 2t) + \\
&+ m_3^2(3s^2 + 4st + 4t^2) + m_2^2(-8m_3^2 s + 3s^2 + 16st + 4t^2)) + m_1^2(48m_3^4 s + \\
&+ s(-3s^2 + 10st + 4t^2) - 2m_2^2(s^2 + 20st + 8t^2) - 2m_3^2(7s^2 + 20st + 8t^2))) + \\
&+ \frac{1}{32(4m_1^2 - s)s}I_{\text{xbox}}\left[X\right](84m_1^6 s + m_1^4(-49s^2 + 24st - 32t^2 - 6m_2^2(s+2t) + \\
&+ 6m_3^2(s+2t)) + s(-2m_2^4 s + s(10m_3^4 + 5m_3^2 s + 7st) + m_2^2(-8m_3^2 s + 5s^2 + 4st + 8t^2)) + \\
&- m_1^2(s(-7s^2 + 34st - 8t^2) + 2m_3^2(11s^2 + 8st + 4t^2) + 2m_2^2(5s^2 + 12t^2))) + \\
&- \frac{1}{64(4m_1^2 - s)s}I_{\text{xbox}}[1](28m_1^8 s - m_1^6(7s^2 + 4st + 32t^2 + 2m_2^2(s+2t) - 2m_3^2(s+2t)) + \\
&- m_1^4(2m_2^2(6s^2 + st + 10t^2) - t(25s^2 + 48st + 16t^2) + m_3^2(52s^2 + 46st + 44t^2)) + \\
&- m_1^2(32m_3^6 s + 2m_2^4 s^2 + 2st(3s^2 + 5st + 2t^2) - 2m_3^4(s^2 + 16st + 16t^2) + m_2^2(-5s^3 + \\
&+ 38s^2 t + 24st^2 + 16t^3) + m_3^2(-13s^3 + 14s^2 t + 8st^2 + 16t^3 - 8m_2^2(s^2 + 10st + 4t^2))) + \\
&+ s(m_3^2 t(10m_3^2 s + 5s^2 + 2st + 4t^2) + 2m_2^4(2m_3^2 s - t(5s + 4t)) + m_2^2(4m_3^4 s + t(13s^2 + \\
&+ 10st + 4t^2) - 2m_3^2(3s^2 + 14st + 4t^2)))) + \dots \tag{5.21}
\end{aligned}
$$

where $\dots$ stands for integrals with few than 7 propagators. The integral reduction at the level of crossed box takes about 22 minutes with our Mathematica code. We also performed the integral reduction of crossed box with doubled propagators, by the same method for the double box case as (3.33). All integral reduction relations obtained by our method have been numerically verified by FIRE [3, 4].

6 Conclusions

In this paper, we present the relation between the on-shell IBPs and the meromorphic one-forms on algebraic curves, for a class of two-loop diagrams: D-dimensional L-loop diagram with $DL - 1$ propagators and one unitarity cut solution. In this case, the unitarity cut has a globally well-defined one-dimensional complex structure on it, and hence the analysis of IBPs relations can be translated into the analysis of complex curves.

By presenting several two-loop examples, planar and non-planar, we show that from the knowledge of algebraic curves, it is very easy to construct an IBP relation which reduces an arbitrary integral to master integrals. No explicit form of elliptic/hyperelliptic function is needed in our method, since only the differential relations of these functions are needed. Our method works for the reduction of integrals with or without doubled propagators.

There are several interesting future directions. In this paper, we mainly consider diagrams of $DL - 1$ propagators without three-point massless vertice. If a $(DL - 1)$-propagator diagram has three-point massless vertices, generically, the unitarity cut is not an irreducible curve but a reducible curve, i.e, union of several irreducible algebraic curves. We find that the IBPs obtained from our method, has a smooth massless limit and the limit forms a subset of IBPs for these diagrams. For example, the massless limit of our method, applied on the massless double box diagram, provides all but 2 IBPs. The missing 2 IBPs contain only low-rank numerators, so can be easily found by other algorithms. So in these cases, our method would greatly speed up the integral reduction process, even if IBPs are not all obtained. In the future, we expect that the algebraic geometry analysis on reducible curves will lead the complete set of on-shell IBPs of these diagrams.

In this paper we studied the maximal cut level, and our algorithm can find the analytic on-shell IBPs very quickly. However, it is well known that to get the subdiagrams coefficents in IBP computation can be difficult and time consuming. Following the ideas presented in this paper we may consider using geometric properties of *algebraic surfaces* to study loop diagrams with an arbitrary number of propagators. It is well known that the algebraic geometry property of surfaces is more complicated than that for curves. However, we expect our approach will be generalized for the surfaces cases, because essentially our method does not depend on the detailed information of elliptic/hyperelliptic functions or integrals. Only the complex structure and differential relations are needed. So the surface cases would be studied following this direction, and to recover the "..." terms in our reduction like (3.27) and (5.21).

Finally, we will study the ϵ-dependent part of the integral reduction, based on our method. In this paper, we consider diagrams with integer-valued spacetime dimension. The ongoing research on two-loop maximal unitarity in dimensional regularization scheme [75], also based on algebraic geometry tools, will help us to understand IBPs with dimensional regularization from a geometric viewpoint.

Acknowledgments

A Rudiments of algebraic curves

In this appendix we give a brief introduction to the mathematical background of algebraic curves used in this paper. The extensive treatment can be found in ref. [34–36].

Definition 1 *A Riemann surface is a connected one-dimensional complex manifold.*

We are mostly interested in compact Riemann surface. Any compact Riemann surface is homeomorphic to a sphere with $g \geq 0$ handles attached, and the number g is called the genus of the Riemann surface. Since the complex dimension is one, we also denote a compact Riemann surface as a complex algebraic curve. However, rigorously speaking, we may need to blow up possible singular points on an algebraic curve to make it a Riemann surface.

Definition 2 *A holomorphic map between Riemann surfaces X and Y is a continuous map $f : X \to Y$ such that for each holomorphic coordinate ϕ_U on U containing x on X and ψ_W defined in a neighbourhood of $f(x)$ on Y, the composition*

$$\psi_W \circ f \circ \phi_U^{-1} \tag{A.1}$$

is holomorphic.

Definition 3 *A meromorphic function f on a Riemann surface X is a holomorphic map to the Riemann sphere $S = \mathbb{C} \cup \{\infty\}$.*

One very useful theorem regarding to the topological properties of algebraic curves is Riemann-Hurwitz theorem. Here we consider the special cases of $f : X \to S$. If in a neighborhood of $P \in X$, P is located at the origin and f has the expansion $f(z) - f(0) \sim z^n$, $n > 1$, then we say P is a *ramified point* of f and n is the ramification index of P. Removing images of *ramification points* under f, we get a Riemann sphere excluding a finite number of points, namely $\hat{S}$. For any point $Q \in \hat{S}$, define that $d(Q) \equiv \# f^{-1}(Q)$, the number of points in the inverse image. d is an integer-valued and continuous function, hence a constant. This constant d is called the degree of f.

Theorem 1 *(Riemann-Hurwitz) Let $f : X \to S$ be a meromorphic function of degree d on a closed connected Riemann surface X. The ramified points are $x_1, \ldots, x_n$, with multiplicity $m_1, \ldots, m_n$. Then the Euler character of X,*

$$\chi(X) = 2d - \sum_{k=1}^{n} (m_k - 1). \tag{A.2}$$

For a compact Riemann surface, the Euler character is related to the genus g, i.e., number of handles as,

$$\chi = 2 - 2g. \tag{A.3}$$

The $g = 0$ compact Riemann surface is a Riemann sphere, while $g = 1$ compact Riemann surface is an elliptic curve (or torus topologically). $g > 1$ cases are more complicated, and we focus a particular class, *hyperelliptic curves*, which is defined as an algebraic curve,

$$\mathcal{C} : y^2 = h(x) \tag{A.4}$$

h is a degree-n polynomial in x with n distinct roots. $\mathcal{C}$ has the genus g, if $d = 2g + 1$ or $d = 2g + 2$, by (A.2). Note that $g = 2$ curve must be hyperelliptic, but not all $g > 2$ curves are hyperelliptic.

In the hyperelliptic case, x and y become meromorphic function with these properties,

- x is a meromorphic function of degree 2 on $\mathcal{C}$,

- y is a meromorphic function of degree n on $\mathcal{C}$,

- $x : \mathcal{C} \to S$ has $2g + 2$ ramified points. If n is even, these points are $(x, y) = (a_i, 0)$ where a_i's are the roots of $h(x)$. If n is odd, these points are $(x, y) = (a_i, 0)$ and the point at infinity.

- Every meromorphic function f on $\mathcal{C}$ can be uniquely written as

$$f = r(x) + y s(x) \tag{A.5}$$

where $r(x)$ and $s(x)$ are rational functions of x.

The last property (A.5) is important for studying the exact meromorphic 1-forms, which play the central role of our integral reduction algorithm.

A.1 Riemann-Roch theorem

We now want to state one of the fundamental theorems of compact Riemann surface X. First, we present several definitions,

Definition 4 *A divisor D on a compact Riemann surface X is a formal sum of points with multiplicities.*

$$D = \sum_{P \in X} n_p P, \tag{A.6}$$

$D \geq 0$ *if and only if $n_P \geq 0$, $\forall P \in X$.*

We can naturally associate a divisor to a meromorphic function f in the following way,

$$(f) = \sum_{P \in X} (\mathrm{ord}_P(f)) P. \tag{A.7}$$

where $\mathrm{ord}_P(f)$ is the leading power of f's Laurent expansion at P. $\deg(D)$ is the degree of the divisor defined as

$$\deg(D) = \sum_{P \in X} n_P. \tag{A.8}$$

$\mathcal{L}(D)$ is the space of meromorphic functions f for which, $(f) + D \geq 0$. We define $l(D) = \dim \mathcal{L}(D)$. Let K be the canonical divisor associated with any meromorphic one form,

$$i(D) \equiv l(K - D). \tag{A.9}$$

We can now state the theorem:

Theorem 2 *(Riemann-Roch) Let X be a compact Riemann surface of genus g and $D \in$ a divisor.*

$$l(D) - i(D) = \deg(D) - g + 1. \tag{A.10}$$

It is clear that If $D < 0$ then $l(D) = 0$, so the Riemann-Roch theorem simplifies as,

$$i(D) = -\deg(D) + g - 1. \tag{A.11}$$

On the other hand, if $\deg D \geq 2g - 2$ then $i(D) = 0$. We have

$$l(D) = \deg(D) - g + 1 \tag{A.12}$$

Theorem 3 *If X is a compact Riemann surface of genus g then*

1. *The space of holomorphic one-forms on X form a finite dimensional vector space of complex dimension g,*

2. *If ω is a meromorphic differential on a Riemann surface X then the number of zeros of ω minus the number of poles, counted with multiplicity is $2g - 2$.*

For the hyperelliptic curve (A.4), we can find an explicit basis of the holomorphic one-forms,

Corollary 1 *The g differentials*

$$\frac{x^j dx}{y}, \qquad j = 0, \ldots, g - 1, \tag{A.13}$$

form a basis of holomorphic differential forms.

We use this basis frequently in our paper for the integral reduction.

Open Access. This article is distributed under the terms of the Creative Commons Attribution License ([CC-BY 4.0](#)), which permits any use, distribution and reproduction in any medium, provided the original author(s) and source are credited.

References

[1] K.G. Chetyrkin and F.V. Tkachov, *Integration by Parts: The Algorithm to Calculate β-functions in 4 Loops*, *Nucl. Phys.* **B 192** (1981) 159 [INSPIRE].

[2] C. Anastasiou and A. Lazopoulos, *Automatic integral reduction for higher order perturbative calculations*, *JHEP* **07** (2004) 046 [hep-ph/0404258] [INSPIRE].

[3] A.V. Smirnov and V.A. Smirnov, *FIRE4, LiteRed and accompanying tools to solve integration by parts relations*, *Comput. Phys. Commun.* **184** (2013) 2820 [arXiv:1302.5885] [INSPIRE].

[4] A.V. Smirnov, *Algorithm FIRE – Feynman Integral REduction*, *JHEP* **10** (2008) 107 [arXiv:0807.3243] [INSPIRE].

[5] A.V. Smirnov, *An Algorithm to construct Grobner bases for solving integration by parts relations*, *JHEP* **04** (2006) 026 [hep-ph/0602078] [INSPIRE].

[6] A. von Manteuffel and C. Studerus, *Reduze 2 - Distributed Feynman Integral Reduction*, arXiv:1201.4330 [INSPIRE].

[7] C. Studerus, *Reduze-Feynman Integral Reduction in C++*, *Comput. Phys. Commun.* **181** (2010) 1293 [arXiv:0912.2546] [INSPIRE].

[8] S. Laporta, *High precision calculation of multiloop Feynman integrals by difference equations*, *Int. J. Mod. Phys.* **A 15** (2000) 5087 [hep-ph/0102033] [INSPIRE].

[9] R.N. Lee, *Presenting LiteRed: a tool for the Loop InTEgrals REDuction*, arXiv:1212.2685 [INSPIRE].

[10] R.N. Lee, *Group structure of the integration-by-part identities and its application to the reduction of multiloop integrals*, *JHEP* **07** (2008) 031 [arXiv:0804.3008] [INSPIRE].

[11] J. Gluza, K. Kajda and D.A. Kosower, *Towards a Basis for Planar Two-Loop Integrals*, *Phys. Rev.* **D 83** (2011) 045012 [arXiv:1009.0472] [INSPIRE].

[12] R.M. Schabinger, *A New Algorithm For The Generation Of Unitarity-Compatible Integration By Parts Relations*, *JHEP* **01** (2012) 077 [arXiv:1111.4220] [INSPIRE].

[13] A. von Manteuffel and R.M. Schabinger, *A novel approach to integration by parts reduction*, *Phys. Lett.* **B 744** (2015) 101 [arXiv:1406.4513] [INSPIRE].

[14] Y. Zhang, *Integration-by-parts identities from the viewpoint of differential geometry*, arXiv:1408.4004 [INSPIRE].

[15] R.N. Lee and A.A. Pomeransky, *Critical points and number of master integrals*, *JHEP* **11** (2013) 165 [arXiv:1308.6676] [INSPIRE].

[16] Z. Bern, L.J. Dixon, D.C. Dunbar and D.A. Kosower, *One loop n point gauge theory amplitudes, unitarity and collinear limits*, *Nucl. Phys.* **B 425** (1994) 217 [hep-ph/9403226] [INSPIRE].

[17] Z. Bern, L.J. Dixon, D.C. Dunbar and D.A. Kosower, *Fusing gauge theory tree amplitudes into loop amplitudes*, *Nucl. Phys.* **B 435** (1995) 59 [hep-ph/9409265] [INSPIRE].

[18] R. Britto, F. Cachazo and B. Feng, *Generalized unitarity and one-loop amplitudes in $N = 4$ super-Yang-Mills*, *Nucl. Phys.* **B 725** (2005) 275 [hep-th/0412103] [INSPIRE].

[19] R. Britto, F. Cachazo and B. Feng, *New recursion relations for tree amplitudes of gluons*, *Nucl. Phys.* **B 715** (2005) 499 [hep-th/0412308] [INSPIRE].

[20] R. Britto, F. Cachazo and B. Feng, *Computing one-loop amplitudes from the holomorphic anomaly of unitarity cuts*, *Phys. Rev.* **D 71** (2005) 025012 [hep-th/0410179] [INSPIRE].

[21] R. Britto, F. Cachazo, B. Feng and E. Witten, *Direct proof of tree-level recursion relation in Yang-Mills theory*, *Phys. Rev. Lett.* **94** (2005) 181602 [hep-th/0501052] [INSPIRE].

[22] R. Britto, E. Buchbinder, F. Cachazo and B. Feng, *One-loop amplitudes of gluons in SQCD*, *Phys. Rev.* **D 72** (2005) 065012 [hep-ph/0503132] [INSPIRE].

[23] C. Anastasiou, R. Britto, B. Feng, Z. Kunszt and P. Mastrolia, *D-dimensional unitarity cut method*, *Phys. Lett.* **B 645** (2007) 213 [hep-ph/0609191] [INSPIRE].

[24] C. Anastasiou, R. Britto, B. Feng, Z. Kunszt and P. Mastrolia, *Unitarity cuts and Reduction to master integrals in d dimensions for one-loop amplitudes*, *JHEP* **03** (2007) 111 [hep-ph/0612277] [INSPIRE].

[25] F. Cachazo, *Holomorphic anomaly of unitarity cuts and one-loop gauge theory amplitudes*, hep-th/0410077 [INSPIRE].

[26] D.A. Kosower and K.J. Larsen, *Maximal Unitarity at Two Loops*, *Phys. Rev.* **D 85** (2012) 045017 [arXiv:1108.1180] [INSPIRE].

[27] H. Johansson, D.A. Kosower and K.J. Larsen, *Two-Loop Maximal Unitarity with External Masses*, *Phys. Rev.* **D 87** (2013) 025030 [arXiv:1208.1754] [INSPIRE].

[28] M. Søgaard, *Global Residues and Two-Loop Hepta-Cuts*, *JHEP* **09** (2013) 116 [arXiv:1306.1496] [INSPIRE].

[29] H. Johansson, D.A. Kosower and K.J. Larsen, *Maximal Unitarity for the Four-Mass Double Box*, *Phys. Rev.* **D 89** (2014) 125010 [arXiv:1308.4632] [INSPIRE].

[30] S. Caron-Huot and K.J. Larsen, *Uniqueness of two-loop master contours*, *JHEP* **10** (2012) 026 [arXiv:1205.0801] [INSPIRE].

[31] M. Søgaard and Y. Zhang, *Multivariate Residues and Maximal Unitarity*, *JHEP* **12** (2013) 008 [arXiv:1310.6006] [INSPIRE].

[32] M. Søgaard and Y. Zhang, *Elliptic Functions and Maximal Unitarity*, *Phys. Rev.* **D 91** (2015) 081701 [`arXiv:1412.5577`] [ɪɴSPIRE].

[33] H. Johansson, D.A. Kosower, K.J. Larsen and M. Søgaard, *Cross-Order Integral Relations from Maximal Cuts*, *Phys. Rev.* **D92** (2015) 025015, [`arXiv:1503.06711`] [ɪɴSPIRE].

[34] P. Griffiths and J. Harris, *Principles of Algebraic Geometry*, Wiley Classics Library, Wiley (2011).

[35] R. Miranda, *Algebraic Curves and Riemann Surfaces*, Dimacs Series in Discrete Mathematics and Theoretical Comput., American Mathematical Society (1995).

[36] H. Farkas and I. Kra, *Riemann Surfaces: With 27 figures*, Graduate Texts in Mathematics, Springer New York, U.S.A. (1992).

[37] G. Ossola, C.G. Papadopoulos and R. Pittau, *Reducing full one-loop amplitudes to scalar integrals at the integrand level*, *Nucl. Phys.* **B 763** (2007) 147 [`hep-ph/0609007`] [ɪɴSPIRE].

[38] G. Ossola, C.G. Papadopoulos and R. Pittau, *CutTools: A Program implementing the OPP reduction method to compute one-loop amplitudes*, *JHEP* **03** (2008) 042 [`arXiv:0711.3596`] [ɪɴSPIRE].

[39] P. Mastrolia and G. Ossola, *On the Integrand-Reduction Method for Two-Loop Scattering Amplitudes*, *JHEP* **11** (2011) 014 [`arXiv:1107.6041`] [ɪɴSPIRE].

[40] S. Badger, H. Frellesvig and Y. Zhang, *An Integrand Reconstruction Method for Three-Loop Amplitudes*, *JHEP* **08** (2012) 065 [`arXiv:1207.2976`] [ɪɴSPIRE].

[41] Y. Zhang, *Integrand-Level Reduction of Loop Amplitudes by Computational Algebraic Geometry Methods*, *JHEP* **09** (2012) 042 [`arXiv:1205.5707`] [ɪɴSPIRE].

[42] P. Mastrolia, E. Mirabella, G. Ossola and T. Peraro, *Scattering Amplitudes from Multivariate Polynomial Division*, *Phys. Lett.* **B 718** (2013) 173 [`arXiv:1205.7087`] [ɪɴSPIRE].

[43] B. Feng and R. Huang, *The classification of two-loop integrand basis in pure four-dimension*, *JHEP* **02** (2013) 117 [`arXiv:1209.3747`] [ɪɴSPIRE].

[44] P. Mastrolia, E. Mirabella, G. Ossola and T. Peraro, *Integrand-Reduction for Two-Loop Scattering Amplitudes through Multivariate Polynomial Division*, *Phys. Rev.* **D 87** (2013) 085026 [`arXiv:1209.4319`] [ɪɴSPIRE].

[45] P. Mastrolia, E. Mirabella, G. Ossola and T. Peraro, *Multiloop Integrand Reduction for Dimensionally Regulated Amplitudes*, *Phys. Lett.* **B 727** (2013) 532 [`arXiv:1307.5832`] [ɪɴSPIRE].

[46] S. Badger, H. Frellesvig and Y. Zhang, *A Two-Loop Five-Gluon Helicity Amplitude in QCD*, *JHEP* **12** (2013) 045 [`arXiv:1310.1051`] [ɪɴSPIRE].

[47] R. Huang and Y. Zhang, *On Genera of Curves from High-loop Generalized Unitarity Cuts*, *JHEP* **04** (2013) 080 [`arXiv:1302.1023`] [ɪɴSPIRE].

[48] J.D. Hauenstein, R. Huang, D. Mehta and Y. Zhang, *Global Structure of Curves from Generalized Unitarity Cut of Three-loop Diagrams*, *JHEP* **02** (2015) 136 [`arXiv:1408.3355`] [ɪɴSPIRE].

[49] M. Sogaard and Y. Zhang, *Unitarity Cuts of Integrals with Doubled Propagators*, *JHEP* **07** (2014) 112 [`arXiv:1403.2463`] [ɪɴSPIRE].

[50] M. Sogaard and Y. Zhang, *Massive Nonplanar Two-Loop Maximal Unitarity*, *JHEP* **12** (2014) 006 [`arXiv:1406.5044`] [ɪɴSPIRE].

[51] D.J. Broadhurst, J. Fleischer and O.V. Tarasov, *Two loop two point functions with masses: Asymptotic expansions and Taylor series, in any dimension*, *Z. Phys.* **C 60** (1993) 287 [hep-ph/9304303] [INSPIRE].

[52] F.A. Berends, M. Buza, M. Böhm and R. Scharf, *Closed expressions for specific massive multiloop selfenergy integrals*, *Z. Phys.* **C 63** (1994) 227 [INSPIRE].

[53] S. Bauberger, M. Böhm, G. Weiglein, F.A. Berends and M. Buza, *Calculation of two-loop self-energies in the electroweak Standard Model*, *Nucl. Phys. Proc. Suppl.* **37B** (1994) 95 [hep-ph/9406404] [INSPIRE].

[54] S. Bauberger, F.A. Berends, M. Böhm and M. Buza, *Analytical and numerical methods for massive two loop selfenergy diagrams*, *Nucl. Phys.* **B 434** (1995) 383 [hep-ph/9409388] [INSPIRE].

[55] S. Bauberger and M. Böhm, *Simple one-dimensional integral representations for two loop selfenergies: The Master diagram*, *Nucl. Phys.* **B 445** (1995) 25 [hep-ph/9501201] [INSPIRE].

[56] M. Caffo, H. Czyz, S. Laporta and E. Remiddi, *The Master differential equations for the two loop sunrise selfmass amplitudes*, *Nuovo Cim.* **A 111** (1998) 365 [hep-th/9805118] [INSPIRE].

[57] S. Groote, J.G. Korner and A.A. Pivovarov, *On the evaluation of sunset - type Feynman diagrams*, *Nucl. Phys.* **B 542** (1999) 515 [hep-ph/9806402] [INSPIRE].

[58] S. Groote, J.G. Korner and A.A. Pivovarov, *A New technique for computing the spectral density of sunset type diagrams: Integral transformation in configuration space*, *Phys. Lett.* **B 443** (1998) 269 [hep-ph/9805224] [INSPIRE].

[59] M. Caffo, H. Czyz and E. Remiddi, *Numerical evaluation of the general massive 2 loop sunrise selfmass master integrals from differential equations*, *Nucl. Phys.* **B 634** (2002) 309 [hep-ph/0203256] [INSPIRE].

[60] S. Laporta and E. Remiddi, *Analytic treatment of the two loop equal mass sunrise graph*, *Nucl. Phys.* **B 704** (2005) 349 [hep-ph/0406160] [INSPIRE].

[61] S. Pozzorini and E. Remiddi, *Precise numerical evaluation of the two loop sunrise graph master integrals in the equal mass case*, *Comput. Phys. Commun.* **175** (2006) 381 [hep-ph/0505041] [INSPIRE].

[62] S. Groote, J.G. Korner and A.A. Pivovarov, *On the evaluation of a certain class of Feynman diagrams in x-space: Sunrise-type topologies at any loop order*, *Annals Phys.* **322** (2007) 2374 [hep-ph/0506286] [INSPIRE].

[63] B.A. Kniehl, A.V. Kotikov, A. Onishchenko and O. Veretin, *Two-loop sunset diagrams with three massive lines*, *Nucl. Phys.* **B 738** (2006) 306 [hep-ph/0510235] [INSPIRE].

[64] S. Groote, J.G. Korner and A.A. Pivovarov, *A Numerical Test of Differential Equations for One- and Two-Loop sunrise Diagrams using Configuration Space Techniques*, *Eur. Phys. J.* **C 72** (2012) 2085 [arXiv:1204.0694] [INSPIRE].

[65] D.H. Bailey, J.M. Borwein, D. Broadhurst and M.L. Glasser, *Elliptic integral evaluations of Bessel moments*, *J. Phys.* **A 41** (2008) 205203 [arXiv:0801.0891] [INSPIRE].

[66] M. Caffo, H. Czyz, M. Gunia and E. Remiddi, *BOKASUN: A Fast and precise numerical program to calculate the Master Integrals of the two-loop sunrise diagrams*, *Comput. Phys. Commun.* **180** (2009) 427 [arXiv:0807.1959] [INSPIRE].

[67] M. Yu. Kalmykov and B.A. Kniehl, *Towards all-order Laurent expansion of generalized hypergeometric functions around rational values of parameters*, *Nucl. Phys.* **B 809** (2009) 365 [arXiv:0807.0567] [INSPIRE].

[68] S. Müller-Stach, S. Weinzierl and R. Zayadeh, *A Second-Order Differential Equation for the Two-Loop Sunrise Graph with Arbitrary Masses*, *Commun. Num. Theor. Phys.* **6** (2012) 203 [arXiv:1112.4360] [INSPIRE].

[69] L. Adams, C. Bogner and S. Weinzierl, *The two-loop sunrise graph with arbitrary masses*, *J. Math. Phys.* **54** (2013) 052303 [arXiv:1302.7004] [INSPIRE].

[70] E. Remiddi and L. Tancredi, *Schouten identities for Feynman graph amplitudes; The Master Integrals for the two-loop massive sunrise graph*, *Nucl. Phys.* **B 880** (2014) 343 [arXiv:1311.3342] [INSPIRE].

[71] S. Bloch and P. Vanhove, *The elliptic dilogarithm for the sunset graph*, arXiv:1309.5865 [INSPIRE].

[72] L. Adams, C. Bogner and S. Weinzierl, *The two-loop sunrise graph in two space-time dimensions with arbitrary masses in terms of elliptic dilogarithms*, *J. Math. Phys.* **55** (2014) 102301 [arXiv:1405.5640] [INSPIRE].

[73] L. Adams, C. Bogner and S. Weinzierl, *The two-loop sunrise integral around four space-time dimensions and generalisations of the Clausen and Glaisher functions towards the elliptic case*, arXiv:1504.03255 [INSPIRE].

[74] W.L. van Neerven and J.A.M. Vermaseren, *LARGE LOOP INTEGRALS*, *Phys. Lett.* **B 137** (1984) 241 [INSPIRE].

[75] L. Kasper and Y. Zhang, *Two-loop Maximal Unitarity in Dimensional Regularization*, to appear (2015).